

Spatial normalization of optical images of the human hand

Urban Simončič^{1,3}, Luka Rogelj¹, Jaka Ostrovršnik², Matija Tomšič², Jošt Stergar^{1,3}, Rok Hren^{1,4}, Matija Milanič^{1,3}

¹Faculty of Mathematics and Physics, University of Ljubljana, Ljubljana, Slovenia

²Department of Rheumatology, University Clinical Center Ljubljana, Ljubljana, Slovenia

³Jožef Stefan Institute, Ljubljana, Slovenia

⁴Institute of Mathematics, Physics, and Mechanics, Ljubljana, Slovenia

E-pošta: urban.simoncic@fmf.uni-lj.si

Abstract. Spatial normalization is an image registration method to coregister images to a previously defined template. It simplifies the analysis of images taken on the same patient or different patients, at different time points or captured with different imaging modalities. The paper presents a spatial normalization method for the human hand, together with a corresponding template of 21 manually and 242 automatically selected anatomical landmarks. Using landmarks and extrapolation technique, the method coregisters images to the template defined as an average position of individual landmarks on all images. The method is tested on 12 healthy human hands by evaluating the mismatch between the ground truth defined with ultrasound-determined landmarks and the ones defined visually using RGB images. The mean registration uncertainty over the hands was 1.4 ± 1.3 mm. The method utility is demonstrated by being successfully applied to 29 arthritic hands with a pathological finger and hand deformation. Spatial normalization of the hand images enables a pixel-wise analysis of multiple hand images of a same patient taken at different time points with the same modality, as well as images of the same patient taken with a different modality and inter-patient comparison.

Keywords: anatomical landmarks, image registration, spatial normalization, atlas

Prostorska normalizacija optičnih slik človeške roke

Prostorska normalizacija je metoda registracije slik za koregistracijo slik na predhodno definirano predlogo. Poenostavlja analizo slik, posnetih z istim bolnikom ali različnimi bolniki v različnih časovnih točkah ali z različnimi načini slikanja. Članek predstavlja metodo prostorske normalizacije za človeško roko skupaj z ustreznimi predlogo 21 ročno in 242 samodejno izbranih anatomskih oznak. Z uporabo oznak in tehnike ekstrapolacije metoda koregistrira slike na predlogo, definirano kot povprečni položaj posameznih oznak na vseh slikah. Metoda je preizkušena na 12 zdravih človeških rokah z vrednotenjem neujemanja med pravimi pozicijami oznak, določenimi z ultrazvokom, in tistimi, ki so vizualno definirane s slikami RGB. Povprečna registracijska negotovost na rokah je bila $1,4 \pm 1,3$ mm. Uporabnost metode je dokazana z uspešno uporabo na 29 artritičnih rokah s patološko deformacijo prsta in roke. Prostorska normalizacija slik rok omogoča analizo na nivoju slikovnih elementov za več slik rok istega bolnika, posnetih ob različnih časovnih točkah z isto modalnostjo, kot tudi slike istega pacienta, posnete z drugačno modalnostjo, in primerjavo med bolniki.

1 INTRODUCTION

Optical imaging of the human skin is of great importance in the detection of various pathological conditions. It is useful in a variety of medical fields with applications

including the monitoring and diagnosis of diseases, such as diabetic ulcer formation, melanoma, and other malignancies, as well as wound healing control [1]. Spectral images of the skin contain data about spatial distributions and concentrations of tissue chromophores, such as oxy- and deoxyhemoglobin, melanin, bilirubin, and carotene [2,3]. The determined tissue properties are visualized as images, in which the enhanced features appear in an arbitrary color [4].

Many optical imaging techniques can be used for imaging human hands. Multispectral imaging of human hands focuses mostly on inflammatory and immunologic disorders that exhibit a subtle color appearance change like scleroderma and dermatomyositis [5]. Near-infrared (NIR) and infrared (IR) images were previously used for visualization of the veins network and its patterns [6]. The method was mainly used for biometric purposes, since the patterns are distinct for each person [7,8].

Most of the recent studies involving human hands imaging are interested in the detection of rheumatoid arthritis (RA) and psoriatic arthritis (PSA). RA and PSA are inflammatory diseases of one or more joints. Arthritis has several phases and leads to deformation and destruction of the affected joints. It has a great impact on the patients' quality of life, therefore an early detection is crucial [9]. Among the methods used for imaging human

hands to detect arthritis are hyperspectral [10] and IR imaging [11].

To ease the analysis of images of the same patient at different time points, possibly including different modalities, or to analyze images of different patients in order to improve automatic diagnostics, spatial normalization is used. It is a method of registering an image to a standard template which is very common in neuroimaging [12,13]. Ideally, it eliminates the intersubject anatomical variability within images and makes a direct comparison possible. A template refers to a representative image of studied anatomical features in a selected coordinate space, which then provides a target to which individual images are aligned. In neurology, it is used to create a universal atlas for the study of various diseases (e.g. PET imaging of brains of patients with dementia). The two most used atlases in neurology are the Talairach space and the Montreal Neurological Institute spaces [14].

Following the lead of neurology, we propose a semi-automatic registration method to enable an anatomically meaningful hand comparison between different subjects. It uses a manual and automatic selection of anatomical landmarks of each hand and an extrapolation technique to wrap the hand to a previously defined template. The method is the first standardized hand atlas coordinate system. It allows reporting hand-imaging results in a standard coordinate system to identify image differences between different groups of subjects on a pixel level, improve the statistical power of analyses and generalize the findings to the population level.

2 METHODS

2.1 Imaging system

The imaging system used in the study involves an RGB camera (Flir, Blackfly BFLY-U3-23S6C) and a custom LED illumination system. The camera is combined with a 12 mm objective (F/1.4 2/3") and a linear polarizer. The field of the view is 27 cm × 17 cm with a resolution of 1920 × 1200 pixels. The images are captured at an integration time of 100 ms. To improve the homogeneity of illumination, LED light strips with diffusers are fixed to the sides of the imaging cage (Figure 1) and directed to the object plane. In order to minimize the specular reflection from the object, linear polarizers are mounted in front of the camera and illuminated in the cross-polarized configuration (90° angle between the camera and LED-strips polarizers). The software for capturing and aligning images is written in Matlab (2020a, MathWorks), with an addition of a Visual C++ and OpenCV library. The system is enclosed in a black cage to eliminate the stray light.

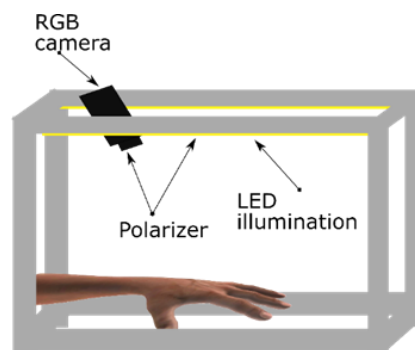


Figure 1: Hand imaging system consisting of an RGB camera and LED illumination; the camera and illumination with polarizers are mounted in the cross-polarized configuration to capture the diffuse light.

2.2 Ultrasonographic evaluation of the joints

For the ultrasonographic (US) assessment of the joints, a Philips Epiq 7 with a 5–18 MHz multi-frequency linear probe is used. A certified European League Against Rheumatism (EULAR) ultrasonographer (JO) performs an US assessment of healthy volunteers and arthritic patients. Firstly, the gray scale and power doppler (frequency of 8.0 MHz and pulse repetition frequency of 400 Hz) US assessment of the MCP and PIP joints in a longitudinal dorsal aspect and with uniform settings in all arthritic patients is performed according to The Outcome Measures in Rheumatoid Arthritis Clinical Trials (OMERACT) Guidelines and scoring system [15,16]. Secondly, spatial locations of the middle of the metacarpophalangeal joint (MCP), proximal interphalangeal joint (PIP) and distal interphalangeal joint (DIP) are determined in healthy volunteers.

2.3 Imaging protocol

Human hands imaging is focusing on three groups of joints – the metacarpophalangeal (MCP), proximal interphalangeal (PIP) and distal interphalangeal joint (DIP). Imaging involves 12 healthy volunteers aged 25 – 40 with fair skin (Fitzpatrick types I-II), both female (8) and male (4) subjects.

First, an experienced rheumatologist examines both hands of each volunteer by US. He marks the location of the DIP, PIP center and MCP joint space (Figure 2) with an alcohol-based marker. The marking serves as a reference point for the analysis of the RGB images. After the US imaging, the hands are imaged with an RGB camera. Subjects put their hands into the imaging cage on the support plate. The operator adjusts the hands to be as flat as possible with the fingers apart from each other and the tip of the middle finger located on a previously defined position. This makes the hands roughly aligned and facilitates a spatial normalization.

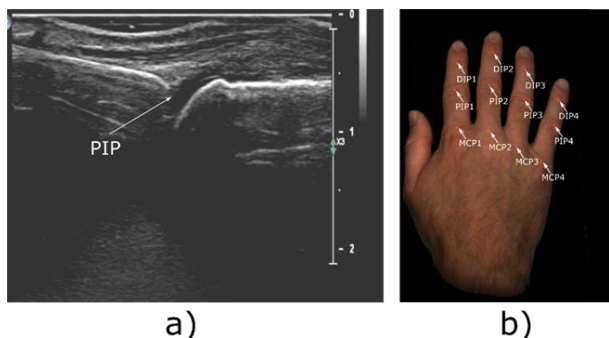


Figure 2: a) An US image of the index finger PIP joint of a 33 year old male volunteer. b) The corresponding RGB image of the volunteer hand with the marked MCP, PIP, and DIP joint spaces based on the US imaging.

Demonstration of the method applicability for patients with joint inflammation is made on 29 patients (23 RA and six PSA, five male and 24 female, age of 30-80). Their hands are imaged by on RGB camera and the recorded images are included in the study.

The procedure is performed according to the Declaration of Helsinki. The applied experimental protocol is approved by the Slovenian National Medical Ethics Committee. An informed consent was obtained from the healthy subjects included in this study.

2.4 Coregistration method

The RGB images are preprocessed by removing the background with a conversion of the RGB to the HSV (hue, saturation, brightness) color space. The hue thresholds and the saturation and brightness values are determined by extracting the binary mask of the hand used for the background removal. The mask is applied to the original RGB image and the pixels at the background locations are set to zero.

The operator manually selected 21 most obvious hand landmarks. They include the DIP, PIP and MCP joints of the four large fingers, interphalangeal (IP) joint of the thumb, fingertips (FT) wrinkle on the palmar side of the thumb and carpometacarpal joints [17] (Figure 3, Step 1, blue crosses).

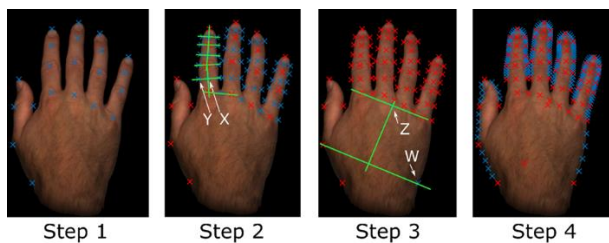


Figure 3: Landmarks manually selected by the operator (Step 1). Landmarks automatically selected (Step 2-4). The red marks present landmarks already selected in the previous steps.

The algorithm assumes a straight line between the joint centers of DIP/PIP, MCP/PIP, DIP/FT and adjacent MCPs (step 2, Figure 3). It calculates the middle points

on the lines between two adjacent joints (X, step 2, Figure 3) and marks them as new landmarks. The perpendicular lines crossing the longitudinal lines in these points are calculated. The edge points on the fingers are extracted (Y, Step 2, Figure 3). Additional 56 points are thus obtained. The points towards the wrist of the hand are also selected (Step 3, Figure 3). The algorithm utilizes the line connecting MCPs of the index and pinkie finger. It calculates the middle point (Z on step 3, Figure 3) and finds a parallel line crossing the IP landmark. It defines a new point on the edge of the hand (W, step 3, Figure 3). Between the adjacent edge points, additional equidistant boundary points are automatically selected (step 4, Figure 3). Overall, 21 manual and 242 automatic points are selected for each hand.

The landmarks determined on the healthy hands are used to create the hand template. The average position of individual landmarks on all images is calculated and used as a reference to which all images are registered. A hand template is a universal human hand outline determined from a healthy hands dataset. Our calculated template is used on both the healthy and arthritic hand (Figure 4).



Figure 4: Outline of all hands (gray lines) and outline of an average hand (black lines).

To coregister a hand to the calculated template, displacements of pixels in the X and Y direction between the template and the hand landmarks are calculated using the equations:

$$\begin{aligned} V_{x,i} &= TL_{x,i} - HL_{x,i} \\ V_{y,i} &= TL_{y,i} - HL_{y,i} \end{aligned} \quad (0)$$

where $V_{x,i}$, $TL_{x,i}$, $HL_{x,i}$, $V_{y,i}$, $TL_{y,i}$ and $HL_{y,i}$ are the i -th displacement vector, i -th template landmark and i -th hand landmark in the X and Y direction, respectively. Using the displacement vectors for all the landmarks, two displacement matrices in the size of the initial RGB image (1920×1200) are created, one for the X and the other for the Y direction. The matrices are created by a 2D extrapolation method designed to extrapolate the missing values on the equidistant grid using the landmark position values. The missing values are found by solving a partial differential equation with a finite difference method, taking into account pixels with a valid value. Method is implemented in Matlab [18]. The used version

of the method (number 4) is based on a partial differential equation assuming that each pixel is elastically connected to its closest neighbors horizontally and vertically.

To obtain coregistered image S , extrapolated displacement matrices V_x and V_y are applied to all the pixels of the original hand image R using the equation:

$$S[i, j] = R[i - V_x[i, j], j - V_y[i, j]]. \quad (2)$$

where i and j are the matrix coordinate indices.

2.5 Coregistration validation

To estimate the registration uncertainty, images are registered to the same template twice. Firstly, the registration is performed by using only the landmarks selected manually on the RGB images (unmarked images) by a blind operator with no previous knowledge about the joint space location. Secondly, the registration is performed using the landmarks determined by a rheumatologist using US (marked images).

The displacement matrices for the marked and unmarked images are subtracted to estimate the registration error. The mean and standard deviation of the registration error indicate the registration uncertainty. The scheme of the coregistration method validation is presented in Figure 5.

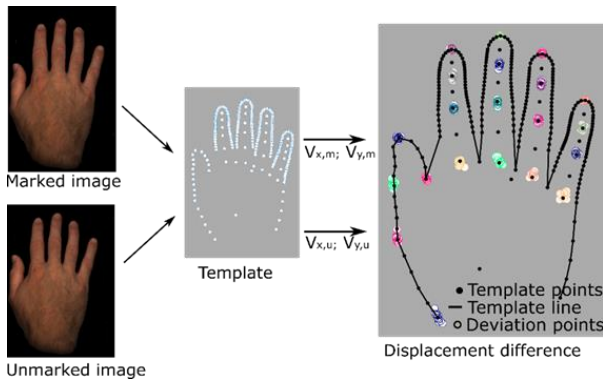


Figure 5: Scheme of the registration procedure of the unmarked and marked image databases to the hand template. Both databases are coregistered to the same template. The difference between them is calculated. It is presented as a deviation of the circles from the template landmark positions.

To create the unmarked images, the original images are modified by exchanging the pixels marked by the rheumatologist with the values interpolated from the nearby clear pixels. This results in an unmarked image enabling an unbiased landmark selection by a blind operator.

3 RESULTS

3.1 Calculation of the hand template

The marked hand images are used for the creation of the hand template, its outline is drawn with a solid line (Figure 6). Each landmark has 12 different locations representing 12 subjects. The black dots represent the

selected landmarks and the ellipses indicate a standard deviation of 1σ over all hands. Both are presented in a standard template space. The standard deviation ellipses are larger for MCPs and for landmarks on the thumb area due to the greater positioning uncertainty of landmarks in those regions. The dispersion of the landmark differences on all fingers is quite similar for most landmark positions. The smallest deviation occurs on the middle finger whose positioning is used for a rough alignment during imaging, while the largest is on the left side of the wrist. The MCP dispersion increases with the distance from the middle finger.

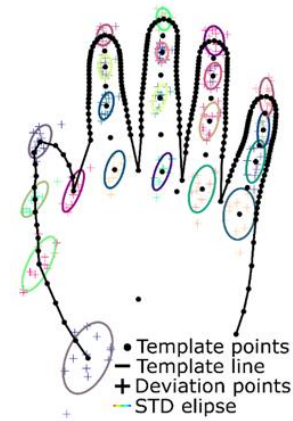


Figure 6: Template points are marked. The manually selected ones have points (+) and a standard deviation of 1σ (ellipse).

3.2 Coregistration of healthy hands

The unmarked and marked images of healthy hands are coregistered to the hand template. Figure 7 shows the differences between the displacement matrices averaged over all the subjects in the X and Y direction. The absolute displacement is calculated using the Pythagorean theorem on the displacement in the X and Y direction. The difference between the absolute displacements is the largest at the areas where the landmarks density is the lowest.

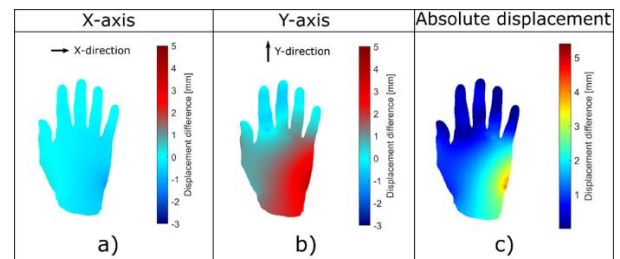


Figure 7: (a,b) Difference between the displacement matrices between the marked and unmarked images in the x and y direction. (c) The absolute displacement differences are calculated by the Pythagorean theorem.

The minimal differences are in the X direction. This means that the US-based and visually-selected landmarks are well aligned in the X direction, consequently

resulting in well aligned automatically-selected points. A blind operator marks the joints in the X direction similarly as the rheumatologist. In the Y direction, the displacement difference is around 1 mm around the fingers and 2-3 mm around the back of the hand. This indicates that the joint cavities on the unmarked images are selected a few millimeters too far in the proximal direction. The largest absolute displacement differences are between MCP4 and the wrist and in the middle of the back hand.

The averaged standard deviation (SD) of the differences and maximum difference (MD) over all 12 subjects is presented in Figure 8. The standard deviation is low in the areas with a higher density of the landmark points (e.g. the right and the middle part of the hand) and high in the areas with a lower density of the landmarks.

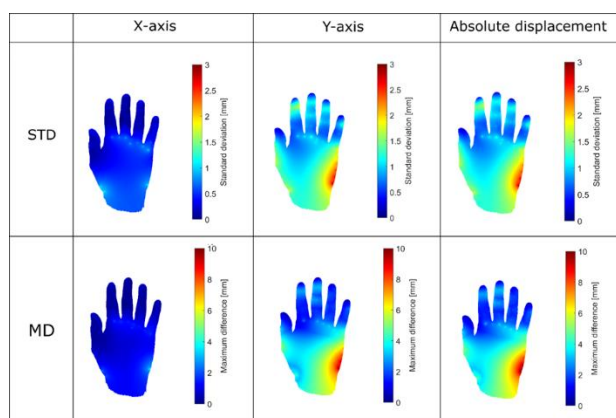


Figure 8: Standard deviation and the maximum difference between the displacements of the marked and unmarked images.

The results show that the standard deviation on the finger area is below 0.7 mm in the X direction and below 1.5 mm in the Y direction. For a more detailed analysis, differences between the displacement matrices and SD averaged over all the subjects are calculated for each finger (Table 1).

Table 1: The mean values and standard deviations for each finger of the displacement differences between the marked and unmarked images.

		Thumb	Index finger	Middle finger	Ring finger	Little finger
Mean X-axis difference [mm]		-0.04±	-0.13±	-0.07±	-0.13±	-0.14±
		0.23	0.27	0.21	0.28	0.35
Mean Y-axis difference [mm]		0.71±	-0.10±	-0.08±	0.57±	0.70±
		1.1	0.83	0.70	0.84	0.87

As for the fingers, the index, middle and ring finger have the lowest displacement differences (Table 1). The best results are observed with the middle finger while the worst with the thumb and small finger. Also, the largest deviations are observed on the thumb and little finger. Since the most important part of our images are finger

joints, all parameters are calculated for individual joints, except for the thumb. The thumb is neglected due to its rotated position and the complexity of defining the area of the joints. The results indicate the largest discrepancies on MCP4 where the mean Y value is up to 2 mm. The blind operator usually marks the MCP joints a few millimeters in the direction towards the wrist, while the DIP joints are usually marked a few millimeters in the direction towards the fingertips. The lowest discrepancies are noticed on PIP and DIP of the middle finger.

The average hand of healthy volunteers is calculated before and after the coregistration (Figure 9). The deviation of the finger areas of different patients is much smaller after the registration.

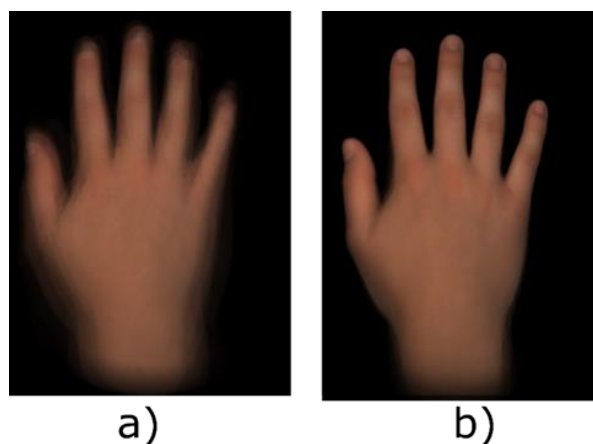


Figure 9: Average hand before a) and after b) the coregistration.

3.3 Arthritic hands

The spatial normalization method is evaluated on the images of 29 patients with RA and PSA. Besides the normal anatomical differences due to the age, size, and prior injuries, the joint swellings and deformations as a consequence of the disease are also present. Stages of the patients' disease are very different, which results in a variety of hand deformations (Figure 10a). Also, every patient has a different combination of affected fingers. Figure 10a shows examples of ten unregistered hands. The arthritic hands have no joints marked, therefore the manual landmarks are chosen based on the RGB image by the operator. The remaining landmarks are automatically determined in the same way as for the healthy hands. Subsequently, the images are coregistered to the previously created template. The spatially normalized results are presented in Figure 10b. The registered hands have less pronounced deformations. The largest difference can be observed on the hands 1, 5, 9 and 10.

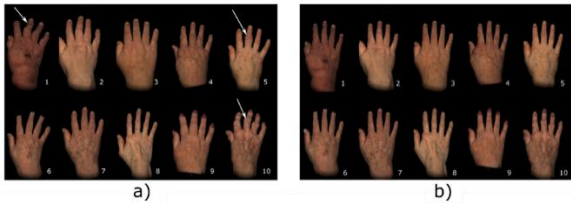


Figure 10: (a) Examples of the unregistered hands affected by arthritis. Various arthritis symptoms can be noticed. Patients 1, 5 and 10 have a severe deformation of the fingers (white arrows). On patient 3, 5 and 9, an inflammation of the fingers can be detected. (b) Samples of the registered hands showing a reduced deformation of hands.

The average hand images of the registered and unregistered hand images are calculated (Figure 11). The registered average hand shows clear edges and joint centers, indicating that the anatomical landmarks of different hands are coregistered with an adequate accuracy.

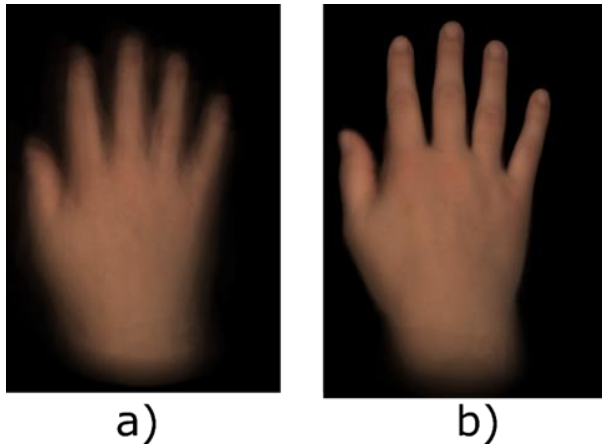


Figure 11: Comparison of an average hand of nonregistered (a) and registered (b) hand images of patients with arthritis.

3.4 A healthy and arthritic hands comparison

To verify that the spatial normalization technique is able to map diseased hands into a template created from healthy hands, “average hands” of healthy subjects and patients are compared. A close examination of both average hands (Figures 9b and 10b) shows that they are visually almost identical, despite the two completely different image databases. The intersection of the two average hands is presented in Figure 12. The healthy and arthritic hands are presented by the green and purple colors, respectively, and the white color represents the intersection of both hands. The arthritic hands average has a greater smearing due to unusual deformations of the hand. However, a great majority of the hands match well. Following the above, the template based on the healthy hands images can also be used for a spatial normalization of the arthritic hands images.



Figure 12: Comparison of the healthy and arthritic average hand images. The healthy and arthritic hands are presented by the green and purple colors, respectively. The white color represents the intersection of both hands..

4 DISCUSSION

A spatial normalization method for optical images of human hands is present. The method involves a combination of manually and automatically selected anatomical landmarks to coregister the hand images to a pre-defined hand template. The registration is performed after a visual selection of the landmarks on an RGB image. The result of a spatial normalisation based on a manual selection of the landmarks was compared to the ground truth registration, where the landmarks are determined by a rheumatologist using US.

The lack of the landmark points between MCP4, wrist, and middle of the back hand results in many different extrapolation possibilities, which causes the largest displacements in that region (Figure 7). Larger SD regions are present around the MCP landmark and the right edge of the hand (Figure 8). To remove the SD peak values near MCPs, the landmarks on these positions are eliminated from the template. The results are not encouraging since the calculated average hand is very smeared.

The best coregistered joints are the DIP and PIP joints with an absolute displacement (AD) between 0.12 mm to 0.7 mm. AD of the worst MCP4 joint is 2.1 mm. The selection of the PIP and DIP joints is easier due to the more prominent wrinkles. On MCPs, the skin is smoother and there is also a visible flexor digitorum superficialis which makes the selection of the joint cavity position even more difficult. Analyzing the results for each finger, the thumb and little finger have the worst mean value and SD due to their rotated position while putting the hand flat on the table.

The method is tested on an arthritic hands. Compared to a healthy hand, the average arthritic hand appears somewhat more blurred (Figure 9 vs. Figure 10). The blurring occurs on soft tissue regions where it takes many different shapes especially in severely deformed hands. However, blurring is not prominent. Therefore, the template calculated from the healthy hand images can be

used also on the arthritic hands images. In our study, only the right hands are imaged. The algorithm can be easily translated for the use on the left hand employing a vertical flipping method.

In our research, coregistration of the RGB hand images is presented. However, the algorithm can be used also on any human hand images where joint centers and hand edges can be extracted, such as hyperspectral imaging and IR imaging. We believe our method can be efficiently used in diagnosing or treatment methods where a comparison between different patients or images of the same patient at different times are needed, and in an early detection of arthritis. Firstly, the method simplifies monitoring the drug efficiency, which is now performed by an experienced radiologist using US. Secondly, calculation of the hand template allows for an easily implemented automatic detection. Any image can be coregistered to the template with a defined coordinate system as they did in [19], in which each coordinate on the final image takes a specific anatomical position.

Reducing the displacement SD between the unmarked and marked fingers (Table 1), requires an altered hand positioning to be obtained by implementing an adequate algorithm, showing the patients how to position their hand before imaging. Such algorithm, developed and tested, will be presented in our future work.

The method can be further improved by adding machine learning (ML) as a landmark selection tool [20,21]. Using ML, the algorithm can be completely automatic and therefore very fast since there would be no operator needed to manually select the anatomical landmarks on every imaged hand.

Another improvement to be made concerns the natural anatomical variability of the human hand. As with pathological changes this variability may further increase, and using an appearance model as a template would be a better option.

Pathological changes along with manual labeling of landmark points are likely to introduce outlier points, which can severely degrade the template coregistration in cases when the landmarks are considered equally relevant. Implementing a matching methodology to consider potential outliers would increase the procedure robustness.

5 CONCLUSIONS

Spatial normalization is an image registration method to analyze images on a pixel level and captured at different time stamps on the same object or between individual subjects. The paper presents a human hand template for a spatial normalization of human hands. Using a semi-automatic selection of anatomical landmarks, hands can be coregistered to a template, presenting well aligned human hands. The results of comparing the registration methods using landmarks defined with US to those defined only by examining the RGB images shows small deviations. The presented method is certainly applicable

to hyperspectral imaging and also to IR when accompanied by an RGB image for the registration.

Despite the very promising results, there are still some challenges to be solved. Though an untrained operator can select the points with an acceptable accuracy, the final goal should be a fully automatic selection of anatomical landmarks from images. As the hands of the arthritic patients may be highly deformed, solving that task would take quite an effort. Irrespective of the above deficiencies, the method can be regarded as a valuable improvement on the analysis of hand image, captured with optical imaging modalities.

REFERENCES

- [1] Zherebtsov E, Dremin V, Popov A, Doronin A, Kurakina D, Kirillin M, Meglinski I and Bykov A 2019 Hyperspectral imaging of human skin aided by artificial neural networks *Biomed. Opt. Express* 10 3545
- [2] Lu G and Fei B 2014 Medical hyperspectral imaging: a review *Journal of Biomedical Optics* 19 010901
- [3] Zherebtsov E, Popov A, Doronin A, Meglinski I and Bykov A 2017 Hyperspectral system for imaging of skin chromophores and blood oxygenation *European Conferences on Biomedical Optics* ed H Dehghani and H Wabnitz (Munich, Germany) p 104120G
- [4] Hashimoto N, Murakami Y, Bautista P A, Yamaguchi M, Obi T, Ohyama N, Uto K and Kosugi Y 2011 Multispectral image enhancement for effective visualization *Opt. Express* 19 9315
- [5] Yamaguchi M, Mitsui M and Murakami M 2005 Multispectral color imaging for dermatology: application in inflammatory and immunologic diseases. *Color and Imaging Conference Final Program and Proceedings* 53–8
- [6] Goel M, Patel S N, Whitmire E, Mariakakis A, Saponas T S, Joshi N, Morris D, Guenter B, Gavrilu M and Borriello G 2015 HyperCam: hyperspectral imaging for ubiquitous computing applications *Proceedings of the 2015 ACM International Joint Conference on Pervasive and Ubiquitous Computing - UbiComp '15 the 2015 ACM International Joint Conference* (Osaka, Japan: ACM Press) pp 145–56
- [7] Geelen B, Spooren N, Tack K, Lambrechts A and Jayapala M 2017 System-level analysis and design for RGB-NIR CMOS camera *SPIE OPTO* ed Y G Soskind and C Olson (San Francisco, California, United States) p 101100B
- [8] Wang L, Leedham G and Cho S-Y 2007 Infrared imaging of hand vein patterns for biometric purposes *IET Computer Vision* 1 113–22
- [9] Majithia V and Geraci S A 2007 Rheumatoid arthritis: diagnosis and management *Am. J. Med.* 120 936–9
- [10] Dolenec R, Laistler E and Milanic M 2019 Assessing spectral imaging of the human finger for detection of arthritis *Biomed. Opt. Express* 10 6555
- [11] Frize M, Adéa C, Payeur P, Di Primio G, Karsh J and Ogungbemile A 2011 Detection of rheumatoid arthritis using infrared imaging *SPIE Medical Imaging* ed B M Dawant and D R Haynor (Lake Buena Vista, Florida) p 79620M
- [12] Mangin J-F, Lebenberg J, Lefranc S, Labra N, Auzias G, Labit M, Guevara M, Mohlberg H, Roca P, Guevara P, Dubois J, Leroy F, Dehaene-Lambertz G, Cachia A, Dickscheid T, Coulon O, Poupon C, Rivière D, Amunts K and Sun Z Y 2016 Spatial normalization of brain images and beyond *Medical Image Analysis* 33 127–33
- [13] Presotto L, Iaccarino L, Sala A, Vanoli E G, Muscio C, Nigri A, Bruzzone M G, Tagliavini F, Gianolli L, Perani D and Bettinardi V 2018 Low-dose CT for the spatial normalization of PET images: A validation procedure for amyloid-PET semi-quantification *NeuroImage: Clinical* 20 153–60

- [14] Chau W and McIntosh A R 2005 The Talairach coordinate of a point in the MNI space: how to interpret it *NeuroImage* 25 408–16
- [15] D'Agostino M-A, Terslev L, Aegerter P, Backhaus M, Balint P, Bruyn G A, Filippucci E, Grassi W, Iagnocco A, Jousse-Joulin S, Kane D, Naredo E, Schmidt W, Szkudlarek M, Conaghan P G and Wakefield R J 2017 Scoring ultrasound synovitis in rheumatoid arthritis: a EULAR-OMERACT ultrasound taskforce — Part 1: definition and development of a standardised, consensus-based scoring system *RMD Open* 3 e000428
- [16] Wakefield R J, Balint P V, Szkudlarek M, Filippucci E, Backhaus M, D'Agostino M-A, Sanchez E N, Iagnocco A, Schmidt W A, Bruyn G A W, Bruyn G, Kane D, O'Connor P J, Manger B, Joshua F, Koski J, Grassi W, Lassere M N D, Swen N, Kainberger F, Klauser A, Ostergaard M, Brown A K, Machold K P, Conaghan P G, and OMERACT 7 Special Interest Group 2005 Musculoskeletal ultrasound including definitions for ultrasonographic pathology *J Rheumatol* 32 2485–7
- [17] Hirt B, Seyhan H, Wagner M and Zumhasch R 2017 *Hand and wrist anatomy and biomechanics: a comprehensive guide* (Stuttgart ; New York: Thieme)
- [18] D'Errico J 2012 inpaint_nans (MATLAB Central File Exchange)
- [19] Mirzaalian H, Lee T K and Hamarneh G 2014 Spatial Normalization of Human Back Images for Dermatological Studies *IEEE Journal of Biomedical and Health Informatics* 18 1494–501
- [20] Payer C, Štern D, Bischof H and Urschler M 2019 Integrating spatial configuration into heatmap regression based CNNs for landmark localization *Medical Image Analysis* 54 207–19
- [21] Urschler M, Ebner T and Štern D 2018 Integrating geometric configuration and appearance information into a unified framework for anatomical landmark localization *Medical Image Analysis* 43 23–36

Urban Simončič graduated in Physics in 2004 and defended his PhD in Physics in 2011 at the Faculty of Mathematics and Physics, University of Ljubljana. He is an assistant professor at the Faculty of Mathematics and Physics, University of Ljubljana. His research interests include biomedical optical imaging and medical image analysis.